Cell Tissue Res (2010) 340:335–346
DOI 10.1007/s00441-010-0958-8

REGULAR ARTICLE

Endoplasmic reticulum accumulation of Kir6.2 without activation of ER stress response in islet cells from adult *Sur1* knockout mice

Ihsane Marhfour · Jean-Christophe Jonas · Joëlle Marchandise · Alberte Lefevre · Jacques Rahier · Christine Sempoux · Yves Guiot

Received: 13 October 2009 / Accepted: 26 February 2010 / Published online: 6 April 2010

Abstract Trafficking of pancreatic K_{ATP} channels to the plasma membrane critically depends on masking the endoplasmic reticulum (ER) retention signals of the SUR1 and Kir6.2 subunits upon their proper assembly into functional hetero-octamers. When expressed in the absence of the partner protein, each subunit might accumulate in the ER and trigger β-cell ER stress and oxidative stress. To test this hypothesis, Kir6.2 localisation, ER ultra-structure and ER-stress- and oxidative-stress-response gene mRNA levels were evaluated in pancreatic endocrine cells from adult wild-type (WT) and *Sur1* knockout (*Sur1*$^{-/-}$) mice. As previously reported, Kir6.2 was mainly expressed on secretory granules and at the plasma membrane of WT islet cells. In contrast, like the ER chaperone calreticulin, Kir6.2 was primarily localised in the rough endoplasmic reticulum (RER) of *Sur1*$^{-/-}$ islet cells. ER retention of Kir6.2 was demonstrated (electron microscopy) by a significant increase in the length and Kir6.2 density of RER in *Sur1*$^{-/-}$ vs WT islet cells. Despite Kir6.2 retention in RER, *Xbp1* mRNA splicing and mRNA levels of preproinsulin and ER-stress-response genes *Bip*, *Edem* and *Gadd153* were similar in WT and *Sur1*$^{-/-}$ islets. However, mRNA levels of the antioxidant enzymes *Sod1*, *Sod2*, *Gpx2* and catalase were significantly up-regulated in *Sur1*$^{-/-}$ islets. Sequestration of Kir6.2 in RER of *Sur1*$^{-/-}$ islet cells is thus associated with an increase in RER length and mild oxidative stress without activation of the classical ER stress response.

Keywords Electron microscopy · ER stress · Immunohistochemistry · Pancreatic islets · Kir6.2 trafficking · Oxidative stress · Sur1 knockout mice

Abbreviations

BiP	Immunoglobulin heavy chain binding protein
CHI	Congenital hyperinsulinism of infancy
Cyp1a1	Cytochrome P450, family 1, subfamily a, polypeptide 1
Edem	Endoplasmic reticulum degradation-enhancer mannosidase alpha-like 1
Fmo1	Flavin monooxygenase 1
Gadd	Growth arrest and DNA damage
Gpx2	Glutathione peroxidase 2
GSIS	Glucose stimulation of insulin secretion
K_{ATP}	ATP-sensitive potassium channel
RER	Rough endoplasmic reticulum
ROS	Reactive oxygen species
Sod1	Superoxide dismutase 1, soluble
Sod2	Superoxide dismutase 2, mitochondrial
SUR1	Sulphonylurea receptor 1
Sur1$^{-/-}$	Sur1 knockout
Tbp	TATA-box binding protein
WT	Wild-type
Xbp1	X-box binding protein 1

This work was supported by grants 3.4616.05 (J. Rahier), 9.4559.04 (C. Sempoux) and 3.4.516.09 (J.C. Jonas; senior associate of FNRS) from the Fonds de la Recherche Scientifique Médicale, FNRS, Belgium) and by an ARC grant 05/10—328 (I.M., C.S. and J.C.J.) from the General Direction of Scientific Research of the French Community of Belgium.

I. Marhfour · J. Marchandise · A. Lefevre · J. Rahier · C. Sempoux · Y. Guiot (✉)
Department of Pathology, Cliniques Universitaires Saint-Luc, Université Catholique de Louvain,
Tour Rosalind Franklin, 10 Avenue Hippocrate,
1200 Brussels, Belgium
e-mail: yves.guiot@uclouvain.be

J.-C. Jonas
Unit of Endocrinology and Metabolism, Faculty of Medicine, Université Catholique de Louvain,
Brussels, Belgium

Introduction

Functional ATP-sensitive potassium (K_{ATP}) channels, which are present in all pancreatic endocrine cells, are hetero-octamers composed of four pore-forming potassium inward rectifier Kir6.2 subunits (encoded by the *Kcnj11* gene) and four regulatory sulphonylurea receptor SUR1 subunits (encoded by the *Abcc8* gene; Inagaki et al. 1995; Clement et al. 1997; Aguilar-Bryan et al. 1998). In insulin-secreting β-cells, these channels set the resting membrane potential and serve as a critical coupling factor between changes in glucose metabolism and membrane electrical activity; therefore, the channels play a key role in the glucose stimulation of insulin secretion (GSIS; Aguilar-Bryan and Bryan 1999; Ashcroft and Gribble 1999). Gain-of-function mutations of *Kir6.2* have been associated with defective GSIS and the development of type 2 diabetes (Gloyn et al. 2005; Flanagan et al. 2007); however, loss-of-function mutations of *Sur1* and *Kir6.2* are the most common cause of congenital hyperinsulinism of infancy (CHI), a disease characterised by inappropriate insulin secretion in the face of severe hypoglycemia in neonates and infants (Thomas et al. 1995, 1996; Flanagan et al. 2009). In most cases, the loss-of-function mutations alter the biogenesis or trafficking of either subunit, which prevents the correct expression of functional K_{ATP} channels at the cell surface (Cartier et al. 2001; Taschenberger et al. 2002; Yan et al. 2004; Marthinet et al. 2005).

Previous studies have convincingly shown that K_{ATP} channel subunits are assembled in the endoplasmic reticulum (ER) by the following mechanism. Because of the presence of an ER-retention signal (consisting of an Arg-Lys-Arg [RKR] tripeptide) in each channel subunit, SUR1 and Kir6.2 cannot exit the ER before complete channel assembly (Zerangue et al. 1999). Under normal conditions, when both subunits are co-expressed and folded correctly, Kir6.2 and SUR1 associate in a configuration that masks their ER-retention signals, allowing trafficking of the complex to the plasma membrane (Inagaki et al. 1995; Zerangue et al. 1999). In contrast, if Kir6.2 or SUR1 is not expressed or cannot fold correctly, the octameric complex does not form and the other channel subunit remains in the ER.

Several groups have investigated the mechanism by which SUR1 supports the functional expression of Kir6.2 in insulin-secreting cell lines (Makhina and Nichols 1998; Sharma et al. 1999; Zerangue et al. 1999). For example, the removal of the RKR ER-retention sequence from the C-terminal end of Kir6.2 has been shown to allow the formation of functional K^+ channels at the plasma membrane in the total absence of SUR1; however, this finding has not been studied in primary β-cells in vivo. Moreover, we still do not know whether, in *Sur1*$^{-/-}$ mice, the ER sequestration of Kir6.2 induces ER stress in endocrine pancreatic cells, as occurs in other diseases in which mutant proteins accumulate in the ER (e.g. in cystic fibrosis patients, islets accumulate misfolded cystic fibrosis transmembrane conductance regulators; Ali 2009). Therefore, we have examined the sub-cellular localisation of Kir6.2 subunits in pancreatic endocrine cells from *Sur1*$^{-/-}$ mice by using both light and electron microscopy and have investigated the potential impact of altered Kir6.2 trafficking on islet stress-response gene expression in these cells.

Materials and methods

Animals *Sur1* knockout (*Sur1*$^{-/-}$) mice (originally provided by J. Bryan, Pacific Northwest Diabetes Research Institute, Seattle, Washington, USA) and C57BL/6 (WT) mice (Animal facility of the Faculty of Medicine, Université Catholique de Louvain) were bred under standard husbandry conditions. All experiments were approved by the local ethics committee and conducted in accordance with the guidelines issued by the National Belgian Animal Care Committee.

Tissue processing for morphological studies Pancreas, heart and brain tissue samples were collected from mature (13±1 months) WT and *Sur1*$^{-/-}$ mice. For light-microscopic analysis, tissues were fixed in 4% formalin (buffered at pH 7.4) for 24 h, routinely processed and embedded in paraffin. For electron microscopy (EM), samples were fixed in 2.5% glutaraldehyde in 0.1 M sodium cacodylate buffer pH 7.4 (Agar Scientific, Essex, UK), post-fixed in 1% osmium tetroxide (OsO_4; Agar Scientific) and embedded with an epoxy medium according to the manufacturer's recommendations (Fluka, Buchs, Switzerland).

Immunodetection For conventional microscopy, sections (5 µm thick) were incubated with rabbit anti-Kir6.2 (1/100; gift from S.L. Shyng, University of California, USA), which was detected by the EnVision peroxidase complex (1 h; Dako, Carpintera, USA) and by 3,3′-diaminobenzidine (DAB; brown deposit; Guiot et al. 2007). For electron microscopy, after the removal of Epon with sodium metaperiodate (Merck, Darmstadt, Germany) and pre-treatment with 0.1% trypsin/0.1% $CaCl_2$ (Sigma-Aldrich, Steinheim, Germany) in phosphate-buffered saline (PBS) for 20 min at 37°C, semi-thin (1 µm thick) or ultra-thin (75 nm) pancreas sections were incubated overnight at 4°C with rabbit anti-Kir6.2 (1/20) or with goat anti-calreticulin (1/100; Santa Cruz, Calif., USA). Semi-thin sections were incubated for 2 h with either an Alexa fluor 594 goat anti-rabbit antibody (1/150; Molecular Probes, Eugene, Ore., USA; red fluorescence) or a swine anti-rabbit fluorescein

isothiocyanate (FITC)-conjugated antibody (1/20; Dako; green fluorescence). Prior to photomicroscopy, the anti-calreticulin antibody was detected by incubating samples with a rabbit anti-goat antibody for 30 min (1/100; Dako) and with an Alexa fluor 594 goat anti-rabbit antibody for 2 h. The sections were imaged with an Axioplan equipped with a camera (Zeiss-Vision, Munich, Germany; camera: Infinity X-21C, Deltapix, Canada). For Kir6.2 immunostaining, ultra-thin sections were incubated for 2 h with goat anti-rabbit IgG-labelled 12-nm colloidal-gold (1:20; Jackson ImmunoResearch, Baltimore, USA), post-fixed in 2% glutaraldehyde in PBS for 10 min, counterstained and then examined by using a Zeiss 109 transmission electron microscope (Zeiss, Oberkochen, Germany). An irrelevant antibody was used as a negative control for the immunogold system (rabbit anti-*Helicobacter pylori*, 1/20; Dako).

Electron-microscopic quantification of basic organelle parameters and Kir6.2 density The endoplasmic reticulum is an eukaryotic organelle that forms a continuous membrane network (or stacks) of tubules, vesicles and cisternae. We use the term lamellar rough endoplasmic reticulum (L-RER) to specify clearly the elongated cisternae of the RER; this term does not refer to the vesicles.

The endocrine cell surface, nuclear surface and length of L-RER were quantified on random microphotographs of WT and *Sur1*$^{-/-}$ islets (seven islets isolated from five mice per group, final magnification: ×7040) by a semi-automatic image analyser system (Videoplan/MOP-3, Zeiss). Using a digital cursor connected to the image analyser, we circled the endocrine cell and the nucleus and underlined the L-RER structure as shown in Fig. 1. Thus, the image analyser calculated the surface of the highlighted areas and the length of the underlined structures. The L-RER measurement was finally expressed in micrometers per 1000 μm^2 endocrine cell surface (α, β and δ denote glucagon, insulin- and somatostatin-containing cells, respectively) to avoid misinterpretation when the cell profile was not completely represented on the micrograph. Before each measurement (length or surface), the image analyser was calibrated to obtain results expressed as micrometers or square micrometers.

The number of insulin granules was manually counted in 60 β-cells isolated from five mice from each group and the number was expressed per 1000 μm^2 endocrine cell area.

The sub-cellular localisation of Kir6.2 was determined on electron micrographs of WT and *Sur1*$^{-/-}$ endocrine cells by counting the number of Kir6.2 immunogold particles over or proximal to the L-RER and the insulin granule areas in 30 cells of four islets from two pancreases per group. The results were expressed as the number of particles per micrometer L-RER length or per insulin granule (modified from Guiot et al. 2007).

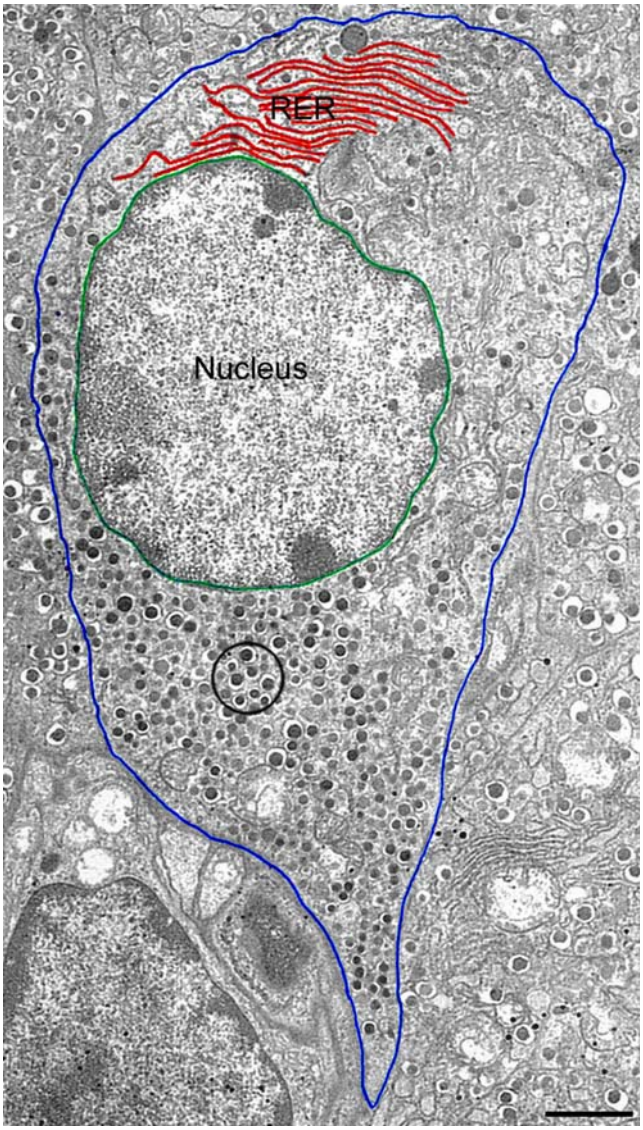

Fig. 1 Quantification by electron microscopy. Electron micrograph of a *Sur1*$^{-/-}$ β-cell (delineated in *blue*) in which the nucleus is surrounded in *green* and the L-RER (lamellar rough endoplasmic reticulum) is highlighted in *red* (*black circle* insulin-containing granules). *Bar* 2 μm

The immunostaining background level was estimated by counting the number of Kir6.2 gold particles in virtual lines (similar to those obtained after delimiting the L-RER) or areas (equivalent to those of insulin granules) both randomly drawn in the cytosol (outside of organelles) of WT mouse β cells.

Pancreatic islet isolation, RNA extraction and cDNA synthesis Pancreatic islets were isolated from the pancreas of old WT and *Sur1*$^{-/-}$ mice (18±1 months; *n*=5 mice/group) by collagenase digestion (Jonas et al. 2003). Next, the islets were micro-dissected and hand-picked under a stereomicroscope to ensure high purity of the preparation. Islet total RNA was extracted, quantified and reverse-transcribed into

cDNA as previously described (Elouil et al. 2007). Control reactions lacking the reverse transcriptase were run in parallel.

Real-time polymerase chain reaction Semi-quantitative real-time polymerase chain reaction (PCR) was performed on an Opticon 2 (Biorad, Hercules, Calif., USA) with SYBR Green Master Mix (Bio-Rad) and 300 or 400 nM gene-specific primers: *proinsulin*, *calreticulin*, *Kir6.2*, *Bip* (*Hsp5*), *Edem*, *Gadd153* (*Ddit3*), *Gpx2*, *catalase*, *Fmo1*, *Cyp1a1*, *Sod1*, *Sod2* and *Tbp* (Table 1). The reaction conditions consisted of 5 min at 95°C followed by 40 cycles: 95°C for 15 s, 60°C for 1 min (except for *Kir6.2* and *Cyp1a1* for which the annealing temperatures were 55 and 59°C, respectively) and 80°C for 30 s. *Tbp* was used as a housekeeping gene. The mRNA expression differences between WT and *Sur1*$^{-/-}$ mice were calculated following the ΔΔCT method (Livak and Schmittgen 2001).

Measurement of Xbp1 mRNA splicing cDNAs corresponding to the unspliced and spliced forms of *Xbp1* mRNA (NM_013842) were amplified simultaneously with *Tbp* cDNA by duplex PCR. The reactions (25 µl) were carried out with 3 µl islet cDNA (20 ng RNA equivalent) in GeneAmp PCR Gold buffer containing 1.25 U AmpliTaq Gold DNA polymerase (Applied Biosystems, Norwalk, Conn., USA), 1.5 mM $MgCl_2$, 200 µM dNTPs and 400nM each primer (sense: 5′-CAAGGGGAGTGGAGTAAGGC-3′, anti-sense: 5′-GGCAACAGTGTCAGAGTCCAT-3′). A 10-min denaturation step at 95°C was followed by 28 cycles of amplification (95°C for 15 s, 62°C for 1 min and 72°C for 1 min) and a 10-min extension step at 72°C. The PCR products were concentrated five-fold before electrophoretic separation and the amplicons were quantified on a 2100 Bioanalyser (Agilent, Waldbronn, Germany). The spliced:total *Xbp1* mRNA ratio was computed as an indicator of *Xbp1* mRNA splicing (Elouil et al 2007).

Statistical analysis All measurements were performed following a blind procedure. Results are expressed as mean±SD or mean±SE. The statistical significance between WT and *Sur1*$^{-/-}$ mice was calculated by a Student *t*-test or a Wilcoxon test. The differences were considered significant if $P<0.05$.

Results

Kir6.2 localisation The specificity of the anti-Kir6.2 antibody was first confirmed by positive immunoreactivity on tissues known to express Kir6.2 protein such as the brain (dentate gyrus area; Fig. 2a), cardiomyocytes (cross-striations with reinforcement at the cell periphery; Fig. 2b) and the endocrine pancreas (islets; Fig. 2c–e). As expected, the pancreatic exocrine tissue remained negative (Fig. 2c).

In WT islets, Kir6.2 immunolabelling was primarily observed in the cytoplasm of endocrine cells (Fig. 2c). However, at a higher magnification, Kir6.2 immunostaining was clearly reinforced at the plasma membrane, which created a mosaic aspect of this immunostaining (Fig. 2d). In contrast, in *Sur1*$^{-/-}$ islets, Kir6.2 immunostaining was only observed in the cell cytoplasm and remained undetectable or at a low level at the plasma membrane (Fig. 2e). Cytoplasmic Kir6.2 staining intensity was similar in both WT and *Sur1*$^{-/-}$ islets.

Table 1 Sequence, final concentration and annealing temperature of oligonucleotide primers used for real-time polymerase chain reaction (for an explanation of the abbreviations, see Abbreviations above)

Name	Sense primer (5′-sequence-3′)	Antisense primer (5′-sequence-3′)	Concentration (nM)	Annealing (°C)
Bip	AACGACCCCTAACAAAAGACAATC	AGGCGGTTTTGGTCATTGGTA	300	60
Calreticulin	TGAGGACTGGGATGAAGAG	GGGGGAGTATTCAGGGTTGT	400	60
Catalase	CATGAATGGCTATGGATCACAC	CAACAGGCAAGTTTTTGATGCC	300	60
Cyp1a1	CTCTCTTTGGTTTGGGCAAG	GACCGCATCTGCACTTGG	400	59
Edem	CTGCCTACACGCCTTCTACTATG	TGGTTGCCTGGTAGAGGAGATA	300	60
Fmo1	CCCAGCATCAAGGAGGTAAA	ACAGCCAGAGTTGGTTTTGG	300	58
Gadd153	ACAGAGGTCACACGCACATC	CCACTCTGTTTCCGTTTCCTAG	300	60
Gpx2	GCATCCTGTCTTTGCCTACC	GCTCGATGTTGATGGTCTGG	300	60
Kir6.2	GTAGGGGACCTCCGAAAGAG	CAGGAAGATGCCGTTACCAC	400	55
Preproinsulin	TCTTCTACACACCCATGTCCC	GGTGCAGCACTGATCCAC	300	60
Sod1	CCAGTGCAGGACCTCATTTTA	CTTGTTTCTCATGGACCACCA	300	60
Sod2	GCCAAGGGAGATGTTACAACT	GAACCTTGGACTCCCACAGA	300	60
Tbp	ACCCTTCACCAATGACTCCTATG	ACTTCGTGCCAGAAATGCTGA	300	60

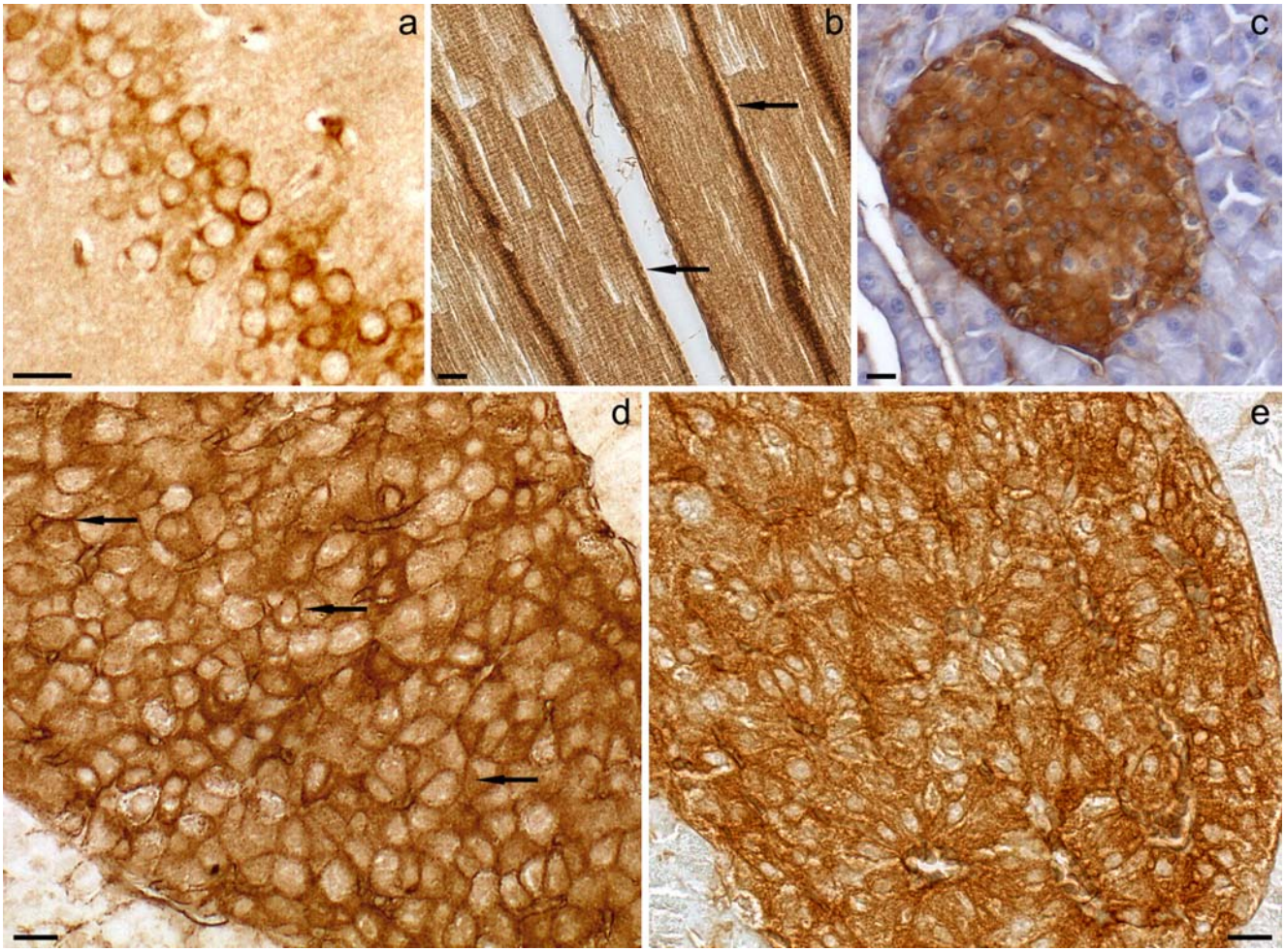

Fig. 2 Specificity of Kir6.2 immunostaining. **a-c** Immunodetection of Kir6.2 in tissue sections from wild-type (WT) mouse brain. **a** Dentate gyrus. ×40. **b** Heart, cardiomyocytes. ×40. **c** Pancreas, islets of Langerhans. ×20. **d**, **e** Kir6.2 immunostaining in, respectively, WT and *Sur1*$^{-/-}$ mouse pancreatic islet cells. ×63. Kir6.2 immunostaining is reinforced at the plasma membrane (*arrows* in **b**, **d**). *Bars* 20 μm

Ultrastructure of endocrine cells Despite their abnormal distribution in *Sur1*$^{-/-}$ islets (Marhfour et al. 2009), endocrine cells were easily identified by the ultrastructural characteristics of their hormone-containing granules in both types of mice (insulin-containing granules, Fig. 3a–b; glucagon-containing granules, Fig. 3c–d). Compared with WT mice, the general ultrastructural features of *Sur1*$^{-/-}$ mouse islet cells (nucleus, mitochondria and granules) were normal. The only obvious difference between WT and *Sur1*$^{-/-}$ islet cell ultrastructure was the higher abundance of L-RER in *Sur1*$^{-/-}$ endocrine cells (Fig. 3b, d).

The endocrine cell profile surface, nuclear surface, number of insulin granules and L-RER length are shown in Table 2. WT β- and non-β-cell profile surfaces were similar to those of *Sur1*$^{-/-}$ matched cells, the profile surface of non-β-cells being smaller than the profile of β-cells. The islet cell nuclear surfaces and the number of insulin granules per 1000 μm^2 of β-cell area were also similar in WT and *Sur1*$^{-/-}$ mice. In contrast, in comparison with WT islet cells, the L-RER length per cell surface in *Sur1*$^{-/-}$ mice was significantly higher in β-cells (approximately four-fold) and δ-cells (approximately two-fold), whereas the length increased 1.5-fold in α-cells (Table 2). However, no obvious dilation of the RER lumen was observed in any of these cell types.

Calreticulin and Kir6.2 expression To test whether the higher L-RER abundance in *Sur1*$^{-/-}$ islets was associated with ER retention of Kir6.2 subunits, we first compared the sub-cellular distribution of Kir6.2 and the ER-specific marker, calreticulin, on pancreatic sections from WT and *Sur1*$^{-/-}$ mice. Calreticulin immunolabelling was weak and homogeneously distributed in the cytoplasm of WT islet cells (Fig. 4a). In comparison, calreticulin staining was more intense in the majority of *Sur1*$^{-/-}$ islet cells and appeared to be preferentially located around the sub-nuclear area, suggesting an abundance of RER in these cells (Fig. 4b). This increase in calreticulin staining occurred

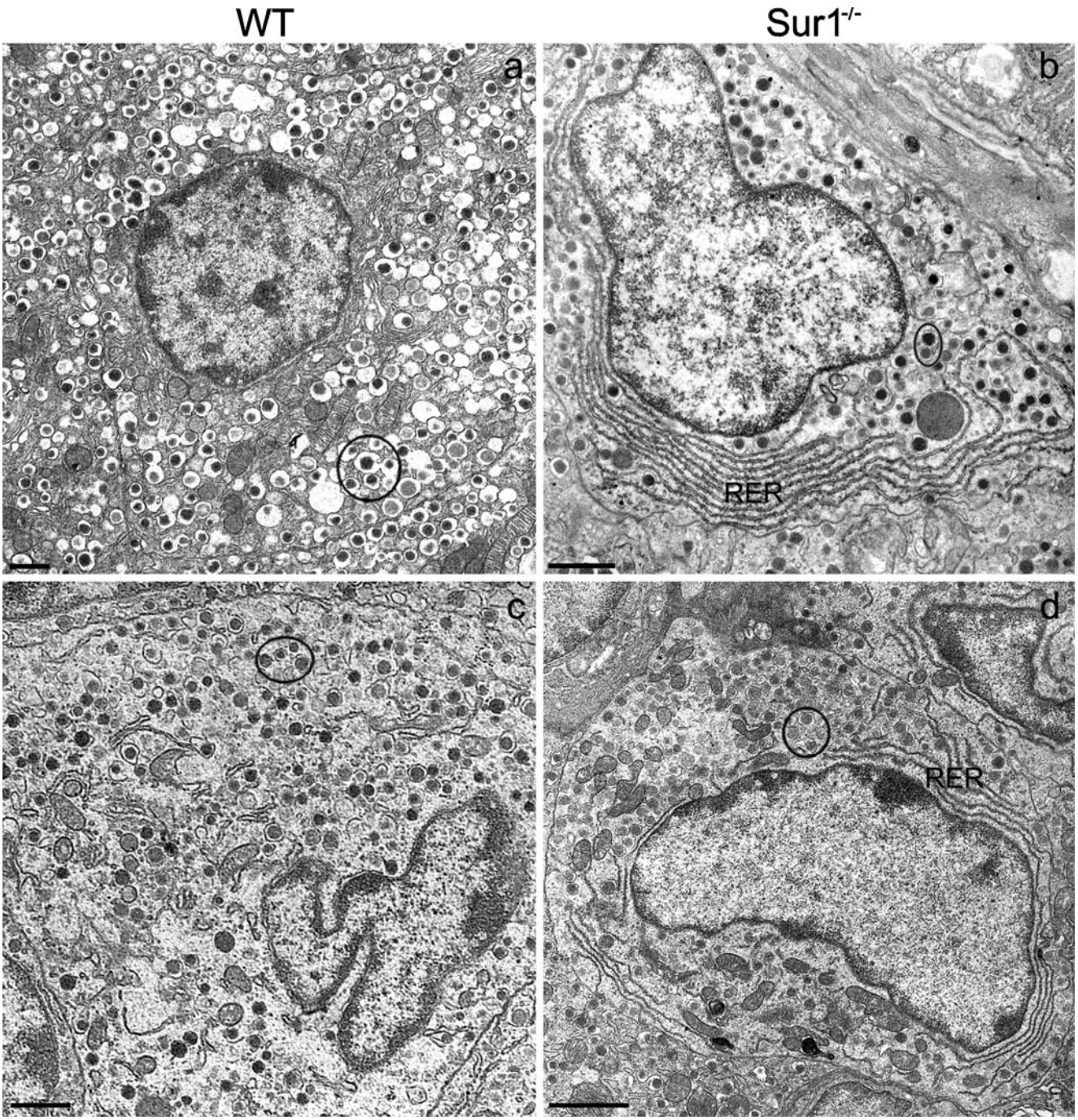

Fig. 3 Ultrastructure of pancreatic β- and α-cells. Electron-microscopic images of typical β-cells (**a**, **b**) and α-cells (**c**, **d**) from WT (**a**, **c**) and *Sur1*$^{-/-}$ (**b**, **d**) mice, identified by their characteristic electron-dense granules (*black circles* insulin- or glucagon-containing granules). The L-RER appeared longer and more developed in β- and α-cells from *Sur1*$^{-/-}$ mice (**b**, **d**) than in WT islet cells (**a**, **c**). ×7040. *Bars*

without changes in calreticulin mRNA levels (1.12±0.13 in *Sur1*$^{-/-}$ vs 1±0.13 in WT islets).

In WT islets, Kir6.2 immunofluorescence was homogenously distributed in the cytoplasm of all islet cells (Fig. 4c). In contrast, the majority of *Sur1*$^{-/-}$ islet cells showed a preferential localisation of Kir6.2 immunofluorescence in the sub-nuclear area (Fig. 4d), corresponding to a higher density of Kir6.2 immunogold particles in the RER (small dark dots; Fig. 5c) in comparison with WT endocrine cells (Fig. 5a). A few Kir6.2 immunogold particles were also observed in insulin granules (Fig. 5c vs Fig. 5a, b) but not in the plasma membrane of *Sur1*$^{-/-}$ islet cells (Fig. 5d); however, Kir6.2 immunoreactivity was positive at the plasma membrane in WT cells (Fig. 5b).

As shown in Fig. 6a, the number of Kir6.2 gold particles per length of L-RER was significantly higher in *Sur1*$^{-/-}$ than

Table 2 Basic cell parameters quantified on electron micrographs of α-, β- and δ-cells from wild-type (*WT*) and *Sur1*$^{-/-}$ mouse islets. Results are means±SD for seven islets from five mice of each group

Measured parameter	α-Cells		β-Cells		δ-Cells	
	WT	*Sur1*$^{-/-}$	WT	*Sur1*$^{-/-}$	WT	*Sur1*$^{-/-}$
Cell profile surface (μm^2)	2277±817	2618±939	3496±1371	3874±1540	2024±841	2221±903
Nuclear profile surface (μm^2)	909±451	943±520	775±359	816±396	543±386	648±441
RER length (μm/1000 μm^2 endocrine cell type)	43±35	67±50	8.5±12.5	33±38**	24±24	50±37*
Granule number (μm/1000 μm^2 endocrine cell type)	–	–	0.46±0.24	0.40±0.14	–	–

*P<0.02 and **P<0.001 for the effect of mouse strain (*Sur1*$^{-/-}$ vs WT); unpaired Student *t*-test

in WT islet cells (P<0.01, Wilcoxon test). The average number of gold particles per insulin-containing granule was significantly lower in *Sur1*$^{-/-}$ than in WT mouse β-cells (P<0.05, Wilcoxon test; Fig. 6b).

The background signal was low outside the L-RER and insulin-containing granules, viz. at least ten-fold lower compared with these specific Kir6.2-positive structures.

The higher density of Kir6.2 in the L-RER of *Sur1*$^{-/-}$ islet cells occurred without significant changes in Kir6.2 mRNA levels (1.21±0.18 in *Sur1*$^{-/-}$ vs 1±0.22 in WT islets).

Gene expression in response to ER stress and oxidative stress The significant increase in L-RER length in addition to a higher Kir6.2 density in *Sur1*$^{-/-}$ islet cells strongly suggested that these cells accumulated Kir6.2 subunits in their ER. To test whether the accumulation of Kir6.2 induced an ER stress response together with oxidative stress, we measured *Xbp1* mRNA splicing, a specific marker of the activation of the unfolded protein response (UPR), in islets isolated from the pancreas of old WT and *Sur1*$^{-/-}$ mice. We also measured the mRNA levels of

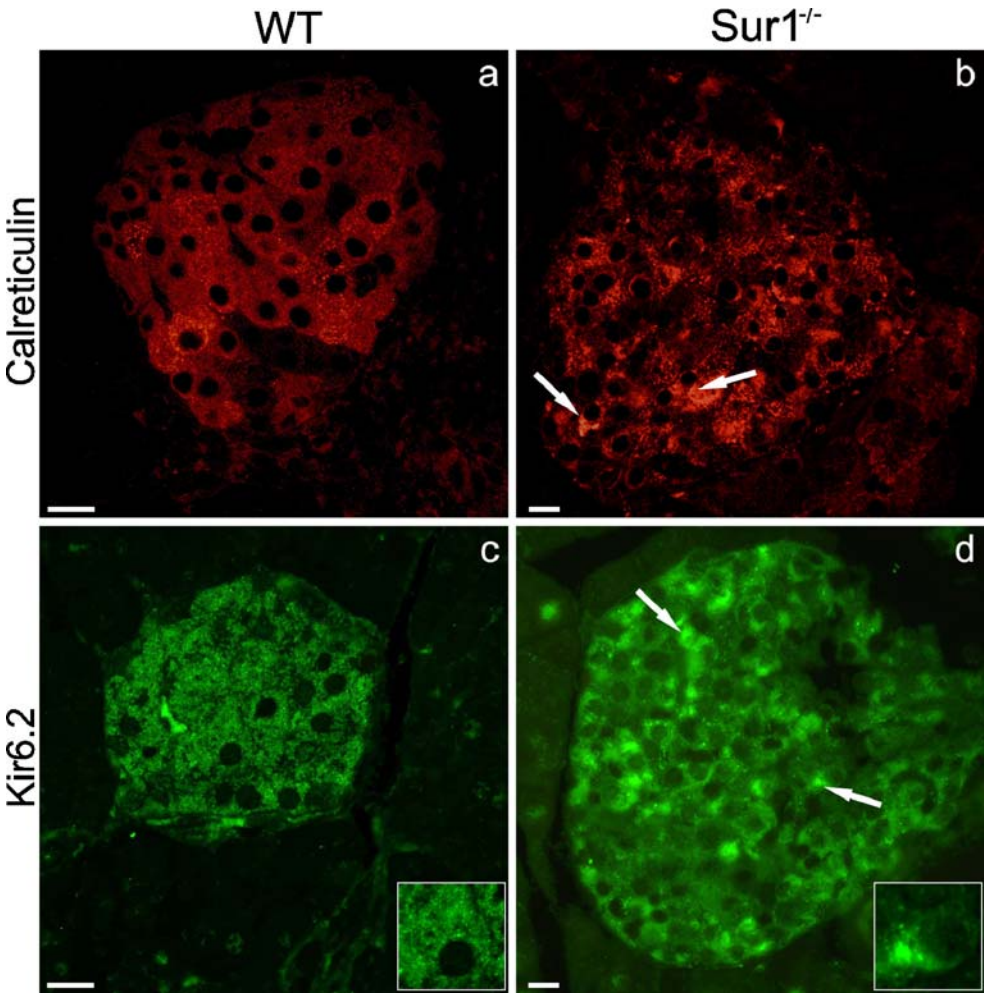

Fig. 4 Calreticulin and Kir6.2 immunolocalisation. Calreticulin (**a**, **b**) and Kir6.2 immunofluorescence in semi-thin sections (**c**, **d**) from WT (**a**, **c**) and *Sur1*$^{-/-}$ (**b**, **d**) islets of Langerhans (*arrows* preferential localisation of fluorescence in the sub-nuclear area in *Sur1*$^{-/-}$ mice; see also *insets* in **c**, **d**). *Bars* 20 μm

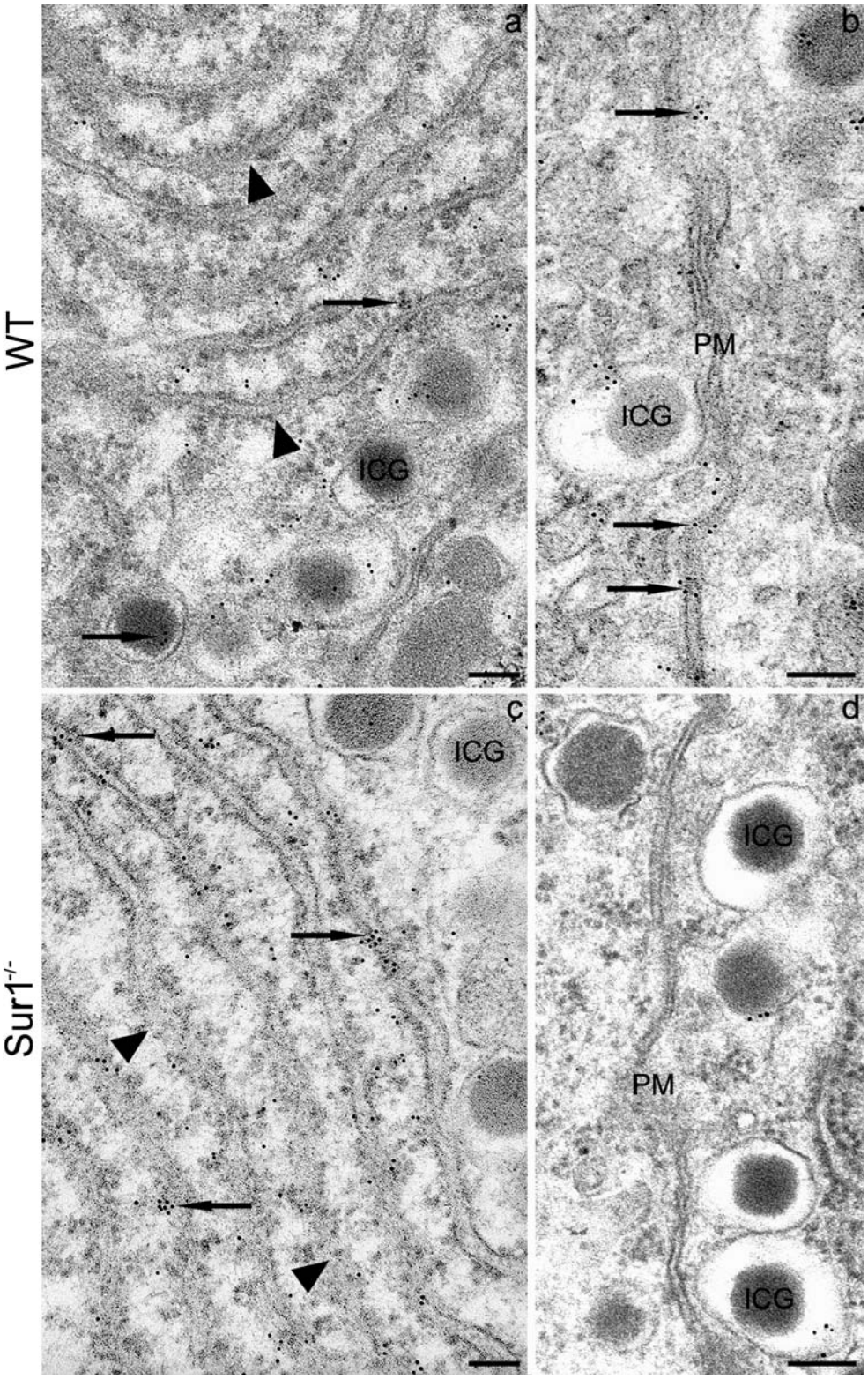

Fig. 5 Sub-cellular localisation of Kir6.2. Immunogold labelling for Kir6.2 in ultra-thin sections from WT (**a**, **b**) and *Sur1*$^{-/-}$ (**c**, **d**) β-cells (*arrowhead* L-RER, *arrow* Kir6.2 immunogold particles, *PM* plasma membrane, *ICG* insulin-containing granules). The β-cells from *Sur1*$^{-/-}$ mice exhibit an increase of gold particle number in the L-RER (**c**) and their absence at the plasma membrane level in comparison with immunogold staining in the WT (**a**, **b**, respectively). *Bars* 120 nm

preproinsulin and of genes known to be up-regulated by ER stress, such as the ER chaperone *Bip* (*Hspa5*), the ER-associated degradation pathway component *Edem* (ER degradation-enhancer mannosidase alpha-like1) and the pro-apoptotic ATF4-target gene *Gadd153* (growth arrest and DNA damage, also known as *Chop* or *Ddit3*). Furthermore, we examined the mRNA levels of genes coding reactive oxygen species (ROS)-producing enzymes such as the cytochrome P450 *Cyp1a1* and the flavin-containing monooxygenase *Fmo1*. In addition, the mRNA

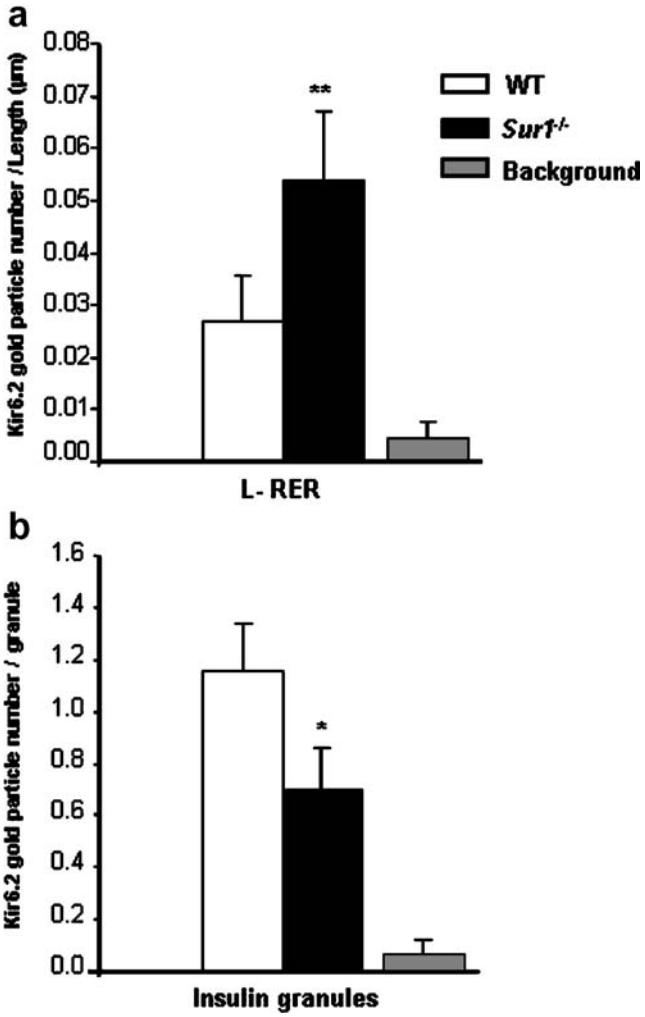

Fig. 6 Quantification of immunogold particles for Kir6.2. The number of Kir6.2 gold particles per micrometer of L-RER length (**a**) and the average number of Kir6.2 gold particles per insulin-containing granule (**b**) were measured in WT and *Sur1*$^{-/-}$ β-cells. Note that the background values were obtained by counting Kir6.2 gold particles in free cytoplasm by means of the same approaches used to quantify the number of particles in the L-RER and in insulin granules. Results are expressed as means±SE (Wilcoxon test: **P*<0.05, ***P*<0.01)

levels of anti-oxidant enzymes such as superoxide dismutase (*Sod1*, *Sod2*), glutathione peroxidase 2 (*Gpx2*) and catalase were analysed.

Xbp1 mRNA splicing (expressed as the ratio of spliced: total *Xbp1* mRNA) was similar in both WT (0.63±0.09) and *Sur1*$^{-/-}$ (0.65±0.05) islets. Moreover, the preproinsulin mRNA levels were similar in WT and *Sur1*$^{-/-}$ islets (0.87± 0.08 in *Sur1*$^{-/-}$ vs 1±0.15 in WT islets). Accordingly, the mRNA levels of *Bip*, *Edem* and *Gadd153* were not significantly increased in *Sur1*$^{-/-}$ vs WT islets (Fig. 7). In *Sur1*$^{-/-}$ islets compared with WT islets, the mRNA levels of *Cyp1a1* were significantly lower and the mRNA levels of *Sod1*, *Sod2*, *Gpx2* and catalase were significantly higher (Fig. 7).

Discussion

The present study demonstrates that, in the absence of SUR1 K_{ATP}-channel regulatory subunits, Kir6.2 channel subunits fail to traffick the endocrine granules and the plasma membrane of pancreatic islet cells. Instead, the Kir6.2 channel subunits accumulate in the L-RER as shown by the following results: (1) the similar sub-cellular localisation of Kir6.2 and the specific ER-marker calreticulin in pancreatic islet cells from *Sur1*$^{-/-}$ but not WT mice and (2) the reduction of Kir6.2 gold particle density in the granular and plasma membrane compartments and its increase in the L-RER compartments of *Sur1*$^{-/-}$ islet cells. Furthermore, we observed that some Kir6.2 immunogold particles were localised not only on the membrane, but also near the membrane. These interpoint distances may be attributable to the physical size of the antibodies, to the size of the particles and/or to their accumulation (Philimonenko et al. 2000). We therefore decided to use small gold particles to avoid the under-detection of extremely close labelling sites and to visualise the sub-celluar localisation accurately.

The localisation of a small number of Kir6.2 gold particles in the granules of *Sur1*$^{-/-}$ islet cells suggests that, despite the absence of SUR1, some Kir6.2 subunits are able to escape the ER compartment and reach insulin granules. We hypothesise that this result may have arisen because of the saturation of the Kir6.2 ER-binding sites in the *Sur1*$^{-/-}$ islet cells. These observations are supported by the current models of K_{ATP} channel assembly based on earlier studies conducted in cells that over-express either or both subunits (Koster et al. 2000; Flagg et al. 2005).

Despite the ER retention of Kir6.2, islet cells from *Sur1*$^{-/-}$ mice do not suffer from classical ER stress: their basic ultrastructural parameters (insulin granule number, nuclear and cell surfaces) are unaffected, the lumen of the RER is not distended, which contrasts with data that has been previously reported in other ER retention diseases (Teckman and Perlmutter 2000; Harding et al. 2001; Ali 2009), and their ER stress response is not activated as shown by the lack of reduction in preproinsulin mRNA levels and the similar mRNA levels of the ER-stress-response genes *Bip*, *Edem* and *Gadd153* in islets from *Sur1*$^{-/-}$ and WT mice (Scheuner and Kaufman 2008). Accordingly, the rate of apoptosis/necrosis of *Sur1*$^{-/-}$ islet cells is not increased, as indicated by the normal volume density of pancreatic endocrine cells and the normal glucose tolerance of old *Sur1*$^{-/-}$ mice (Seghers et al. 2000; Nenquin et al. 2004; Szollosi et al. 2007; Marhfour et al. 2009). Therefore, these results markedly contrast with the increase in β-cell apoptosis and the rapid development of diabetes observed in several models in which β-cells are exposed to sustained activation of their ER stress response

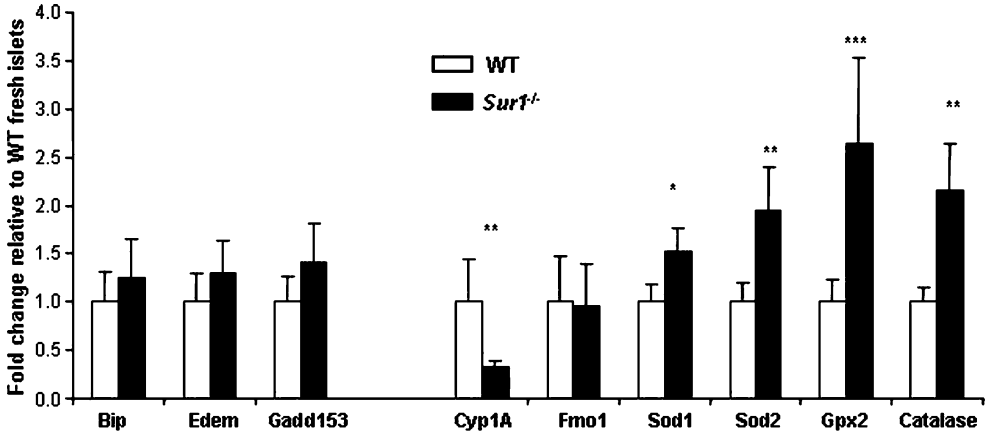

Fig. 7 mRNA levels of ER-stress- and oxidative-stress-response genes. The mRNA levels of several ER-stress-response genes (*Bip*, *Edem* and *Gadd153*), reactive oxygen species (ROS)-producing enzymes (*Cyp1a1*, *Fmo1*) and anti-oxidant enzymes (*Sod1*, *Sod2*, *Gpx2* and catalase) were measured by real-time reverse transcription with the polymerase chain reaction in islets freshly isolated from WT and *Sur1*$^{-/-}$ mice. Gene/*Tbp* mRNA ratios (means±SD) are expressed relative to the ratio measured in WT islets. **P*<0.05, ***P*<0.02, ****P*<0.01 vs WT islets, unpaired Student *t*-test

(e.g. *Perk*$^{-/-}$ mice, Akita mice; Harding et al. 2001; Oyadomari et al. 2002).

Although we have seen no classical signs of ER stress activation, the L-RER content of β- and δ-cells is significantly higher in *Sur1*$^{-/-}$ vs WT mice. For example, in *Sur1*$^{-/-}$ islet cells, calreticulin staining is more intense and preferentially localised in the sub-nuclear area and L-RER length is increased, as shown by electron microscopy. Interestingly, the increase in calreticulin protein levels in *Sur1*$^{-/-}$ vs WT islets occurs without significant changes in calreticulin mRNA levels. Taking into account the theoretical model of Kir6.2 and SUR1 subunit assembly (Zerangue et al. 1999), our results suggest that islet cells from *Sur1*$^{-/-}$ mice are able to compensate for the ER retention of Kir6.2 by increasing the length and Kir6.2 density of the L-RER without sustained activation of the ER stress response. However, our results do not exclude the possibility that the ER stress response is transiently activated to a larger extent in *Sur1*$^{-/-}$ vs WT mice during the early stages of islet cell differentiation. This type of ER adaptation probably requires a transient increase in the biosynthesis of ER constituents such as membrane lipids and ER proteins including calreticulin and other chaperones. However, the mechanism controlling the persistence of this ER adaptation response without sustained increases in the mRNA levels of genes coding ER protein constituents is unknown.

Despite the lack of activation of classical ER stress responses, the mRNA levels of *Cyp1a1*, which is involved in ROS production, are decreased in *Sur1*$^{-/-}$ vs WT islets; however, the mRNA levels of antioxidant enzymes *Sod1*, *Sod2*, *Gpx2* and catalase are significantly increased in *Sur1*$^{-/-}$ vs WT islets. These changes in gene expression are similar to the changes induced upon cell adaptation to mild oxidative stress (Morel and Barouki 1999; Afonso et al. 2007) suggesting that *Sur1*$^{-/-}$ islets are exposed to higher levels of oxidative stress than WT islets. The cause of this oxidative stress is not known but most likely does not result from ER stress. Nevertheless, the adaptive changes in the gene expression of *Sur1*$^{-/-}$ islets may trigger protection against subsequent oxidative stress (as recently shown in islets isolated from diabetic Goto-Kakizaki rats of the Paris colony; Lacraz et al. 2009); therefore, these changes may contribute to the lack of a detectable increase in β-cell apoptosis in *Sur1*$^{-/-}$ vs WT mice.

Although the use of *Sur1*$^{-/-}$ mice is clearly appropriate in order to assess the impact of a lack of SUR1 on Kir6.2 subcellular localisation and ER-stress-response activation in pancreatic β-cells in vivo, the present findings cannot be extrapolated to β-cells from patients with CHI. It has been demonstrated that, despite the total absence of functional K_{ATP} channels, islet β-cells from *Kir6.2*$^{-/-}$ and *Sur1*$^{-/-}$ mice do not hyper-secrete insulin in vivo (Miki et al. 1998; Seghers et al. 2000; Nenquin et al. 2004; Szollosi et al. 2007); however, β-cells from CHI infants hyper-secrete insulin even in the presence of hypoglycaemia (Aynsley-Green et al. 1981; Dunne et al. 2004). Accordingly, whereas *Sur1*$^{-/-}$ β-cells have apparently normal nuclear and cell surface morphology and the same number of insulin granules and proinsulin mRNA levels as WT islets (Marhfour et al. 2009; present study), β-cells from CHI infants display many alterations characteristic of hyper-functioning β-cells such as abnormally large nuclei, abundant cytoplasm, greater cell size, high proinsulin (in the Golgi area) and low insulin content (Rahier et al. 1984, 2000; Sempoux et al. 1998, 2003).

An abundant RER, without no dilation of the lumen, has been recently observed in the diffuse form of CHI (J. Rahier, personal data). Unfortunately, this abundance can be attributed to various causes, such as the hyperfunctional

state, the accumulation of the mutated K_{ATP} subunits (as the present work has revealed in *Sur1*$^{-/-}$ mice) or both. Moreover, no information has been reported concerning the ER-stress-response and the oxidative-stress-response gene expression in islet cells from CHI patients.

Based on the physiological and morphological differences observed between K_{ATP}-channel deficient mouse models (Kir6.2G132S, *Kir6.2*$^{-/-}$ and *Sur1*$^{-/-}$: Miki et al. 1997, 1998; Seghers et al. 2000; Marhfour et al. 2009), we are tempted to speculate that the ER-stress-response and oxidative-stress-response gene expression in islet cells from CHI patients vary according to the type of mutation involved. Thus, mutations that prevent the expression of one channel subunit may only trigger mild ER stress and oxidative stress. In contrast, mutations that cause misfolding of one of the channel subunits and its accumulation in the ER may trigger stronger ER stress and oxidative stress and negatively affect the islet cell mass, which contributes to the gradual transition from CHI to diabetes as described in some CHI patients (initially treated with diazoxide; Glaser et al. 1999; Nichols et al. 2007).

In conclusion, a lack of SUR1 expression in *Sur1*$^{-/-}$ mice leads to a strong reduction of Kir6.2 on the granules and plasma membrane of pancreatic islet cells; however, Kir6.2 accumulates on the L-RER. Such sequestration of Kir6.2 in the RER is associated with an increase in RER length and mild oxidative stress without activation of the classical ER stress response.

Acknowledgments We thank J. Bryan (Pacific Northwest Diabetes Research Institute, Seattle, Washington, USA) and J.C. Henquin (Unit of Endocrinology and Metabolism, Faculty of Medicine, Université Catholique de Louvain, Brussels, Belgium) for providing the *Sur1*$^{-/-}$ mice. We also thank S.L. Shyng (University of California, USA) for the gift of the Kir6.2 antibody and S. Lagasse for expert technical assistance.

References

Afonso V, Champy R, Mitrovic D, Collin P, Lomri A (2007) Reactive oxygen species and superoxide dismutases: role in joint diseases. Joint Bone Spine 74:324–329

Aguilar-Bryan L, Bryan J (1999) Molecular biology of adenosine trisphosphate-sensitive potassium channels. Endocr Rev 20:101–135

Aguilar-Bryan L, Clement JP 4th, Gonzalez G, Kunjilwar K, Babenko A, Bryan J (1998) Toward understanding the assembly and structure of K_{ATP} channels. Physiol Rev 78:227–245

Ali BR (2009) Is cystic fibrosis-related diabetes an apoptotic consequence of ER stress in pancreatic cells? Med Hypotheses 72:55–57

Ashcroft FM, Gribble FM (1999) ATP-sensitive K^+ channels and insulin secretion: their role in health and disease. Diabetologia 42:903–919

Aynsley-Green A, Bloom PJM, SR GMH, Keeling J, Ashcroft SJH, Turner RC, Baum JD (1981) Nesidioblastosis of the pancreas: definition of the syndrome and the management of the severe neonatal hyperinsulinemic hypoglycemia. Am J Dis Child 56:496–508

Cartier EA, Conti LR, Vandenberg CA, Shyng SL (2001) Defective trafficking and function of K_{ATP} channels caused by a sulfonylurea receptor 1 mutation associated with persistent hyperinsulinemic hypoglycemia of infancy. Proc Natl Acad Sci USA 98:2882–2887

Clement JP 4th, Kunjilwar K, Gonzalez G, Schwanstecher M, Panten U, Aguilar-Bryan L, Bryan J (1997) Association and stoichiometry of K_{ATP} channel subunits. Neuron 18:827–838

Dunne MJ, Cosgrove KE, Shepherd RM, Aynsley-Green A, Lindley KJ (2004) Hyperinsulinism in infancy: from basic science to clinical disease. Physiol Rev 84:239–275

Elouil H, Bensellam M, Guiot Y, Vander Mierde D, Pascal SM, Schuit FC, Jonas JC (2007) Acute nutrient regulation of the unfolded protein response and integrated stress response in cultured rat pancreatic islets. Diabetologia 50:1442–1452

Flagg TP, Remedi MS, Masia R, Gomes J, McLerie M, Loptain AN, Nichols CG (2005) Transgenic overexpression of SUR1 in the heart suppresses sarcolemmal K(ATP). J Mol Cell Cardiol 39:647–656

Flanagan SE, Patch AM, Mackay DJ, Edghill EL, Gloyn AL, Robinson D, Shield JP, Temple K, Ellard S, Hattersley AT (2007) Mutations in ATP-sensitive K^+ channel genes cause transient neonatal diabetes and permanent diabetes in childhood or adulthood. Diabetes 56:1930–1937

Flanagan SE, Clauin S, Bellanné-Chantelot C, Lonlay P de, Harries LW, Gloyn AL, Ellard S (2009) Update of mutations in the genes encoding the pancreatic beta-cell K(ATP) channel subunits Kir6.2 (KCNJ11) and sulfonylurea receptor 1 (ABCC8) in diabetes mellitus and hyperinsulinism. Hum Mutat 30:170–180

Glaser B, Ryan F, Donath M, Landau H, Stanley CA, Baker L, Barton DE, Thornton PS (1999) Hyperinsulinism caused by paternal-specific inheritance of a recessive mutation in the sulfonylurea-receptor gene. Diabetes 48:1652–1657

Gloyn AL, Reimann F, Girard C, Edghill EL, Proks P, Pearson ER, Temple IK, Mackay DJ, Shield JP, Freedenberg D, Noyes K, Ellard S, Ashcroft FM, Gribble FM, Hattersley AT (2005) Relapsing diabetes can result from moderately activating mutations in KCNJ11. Hum Mol Genet 14:925–934

Guiot Y, Stevens M, Marhfour I, Stiernet P, Mikhailov M, Ashcroft SJH, Rahier J, Henquin JC, Sempoux C (2007) Morphological localization of sulfonylurea receptor 1 in endocrine cells of human, mouse and rat pancreas. Diabetologia 50:1889–1899

Harding HP, Zeng H, Zhang Y, Jungries R, Chung P, Plesken H, Sabatini DD, Ron D (2001) Diabetes mellitus and exocrine pancreatic dysfunction in perk$^{-/-}$ mice reveals a role for translational control in secretory cell survival. Mol Cell 7:1153–1163

Inagaki N, Gonoi T, Clement JP 4th, Namba N, Inazawa J, Gonzalez G, Aguilar-Bryan L, Seino S, Bryan J (1995) Reconstitution of I_{KATP}: an inward rectifier subunit plus the sulfonylurea receptor. Science 270:1166–1170

Jonas JC, Guiot Y, Rahier J, Henquin JC (2003) Haeme-oxygenase 1 expression in rat pancreatic beta cells is stimulated by supra-physiological glucose concentrations and by cyclic AMP. Diabetologia 46:1234–1244

Koster JC, Marchall BA, Ensor N, Corbett JA, Nichols CG (2000) Target overactivity of β cell K_{ATP} channels induces profound neonatal diabetes. Cell 100:645–654

Lacraz G, Figeac F, Movassat J, Kassis N, Coulaud J, Galinier A, Leloup C, Bailbé D, Homo-Delarche F, Portha B (2009) Diabetic beta-cells can achieve self-protection against oxidative stress through an adaptive up-regulation of their antioxidant defenses. PLoS ONE 4:e6500

Livak KJ, Schmittgen TD (2001) Analysis of relative gene expression data using real-time quantitative PCR and the $2_T^{-\Delta\Delta C}$ method. Methods 25:402–408

Makhina EN, Nichols CG (1998) Independent trafficking of K_{ATP} channel subunits to the plasma membrane. J Biol Chem 273:3369–3374

Marhfour I, Moulin P, Marchandise J, Rahier J, Sempoux C, Guiot Y (2009) Impact of Sur1 gene inactivation on the morphology of mouse pancreatic endocrine tissue. Cell Tissue Res 335:505–515

Marthinet E, Bloc A, Oka Y, Tanizawa Y, Wehrle-Haller B, Bancila V, Dubuis JM, Philippe J, Schwitzgebel VM (2005) Severe congenital hyperinsulinism caused by a mutation in the Kir6.2 subunit of the adenosine triphosphate-sensitive potassium channel impairing trafficking and function. J Clin Endocrinol Metab 90:5401–5406

Miki T, Tashiro F, Iwanaga T, Nagashima K, Yoshitomi H, Aihara H, Nitta Y, Gonoi T, Inagaki N, Miyazaki J, Seino S (1997) Abnormalities of pancreatic islets by targeted expression of a dominant-negative KATP channel. Proc Natl Acad Sci USA 94:11969–11973

Miki T, Nagashima K, Tashiro F, Kotake K, Yoshitomi H, Tamamoto A, Gonoi T, Iwanaga T, Miyazaki J, Seino S (1998) Defective insulin secretion and enhanced insulin action in KATP channel-deficient mice. Proc Natl Acad Sci USA 95:10402–10406

Morel Y, Barouki R (1999) Repression of gene expression by oxidative stress. Biochem J 342:481–496

Nenquin M, Szollosi A, Aguillar-Bryan L, Bryan J, Henquin JC (2004) Both triggering and amplifying pathways contribute to fuel-induced insulin secretion in the absence of sulfonylurea receptor-1 in pancreatic beta-cells. J Biol Chem 279:32316–32324

Nichols CG, Koster JC, Remedi MS (2007) Beta-cell hyperexcitability: from hyperinsulinism to diabetes. Diabetes Obes Metab 9 (Suppl 2):81–88

Oyadomari S, Koizumi A, Takeda K, Gotoh T, Akira S, Araki E, Mori M (2002) Targeted disruption of the Chop gene delays endoplasmic reticulum stress-mediated diabetes. J Clin Invest 109:525–532

Philimonenko A, Janacek J, Hozak P (2000) Statistical evaluation of colocalization patterns in immunogold labelling experiments. J Struct Biol 132:201–210

Rahier J, Fält K, Müntefering H, Becker K, Gepts W, Falkmer S (1984) The basic structural lesion of persistent neonatal hypoglycaemia with hyperinsulinism: deficiency of pancreatic D cells or hyperactivity of B cells? Diabetologia 26:282–289

Rahier J, Guiot Y, Sempoux C (2000) Persistent hyperinsulinaemic hypoglycaemia of infancy: a heterogeneous syndrome unrelated to nesidioblastosis. Arch Dis Child Fetal Neonatal Ed 82:F108–F112

Scheuner D, Kaufman RJ (2008) The unfolded protein response: a pathway that links insulin demand with β-cell failure and diabetes. Endocr Rev 29:317–333

Seghers V, Nakazaki M, DeMayo F, Aguillar-Bryan L, Bryan J (2000) Sur1 knockout mice: a model for K_{ATP} channel-independent regulation of insulin secretion. J Biol Chem 275:9270–9277

Sempoux C, Guiot Y, Lefèvre A, Nihoul-Fékété C, Jaubert F, Saudubray JM, Rahier J (1998) Neonatal hyperinsulinaemic hypoglycaemia: heterogeneity of the syndrome and keys for differential diagnosis. J Clin Endocrinol Metab 83:1455–1461

Sempoux C, Guiot Y, Dahan K, Moulin P, Stevens M, Lambot V, Lonlay P de, Fournet JC, Junien C, Jaubert F, Nihoul-Fekete C, Saudubray JM, Rahier J (2003) The focal form of persistent hyperinsulinaemic hypoglycaemia of infancy: morphological and molecular studies show structural and functional differences with insulinoma. Diabetes 52:784–794

Sharma N, Crane A, Clement JP 4th, Gonzalez G, Babenko AP, Bryan J, Aguilar-Bryan L (1999) The C terminus of SUR1 is required for trafficking of K_{ATP} channels. J Biol Chem 274:20628–20632

Szollosi A, Nenquin M, Henquin JC (2007) Overnight culture unmasks glucose-induced insulin secretion in mouse islets lacking ATP-sensitive K^+ channels by improving the triggering Ca^{2+} signal. J Biol Chem 282:14768–14776

Taschenberger G, Mougey A, Shen S, Lester LB, LaFranchi S, Shyng SL (2002) Identification of a familial hyperinsulinism-causing mutation in the sulfonylurea receptor 1 that prevents normal trafficking and function of K_{ATP} channels. J Biol Chem 277:17139–17146

Teckman JH, Perlmutter DH (2000) Retention of mutant alpha(1)-antitrypsin Z in endoplasmic reticulum is associated with an autophagic response. Am J Physiol Gastrointest Liver Physiol 279:G961–G974

Thomas PM, Cote GJ, Wohllk N, Haddad B, Mathew PM, Rabl W, Aguilar-Bryan L, Gagel RF, Bryan J (1995) Mutations in the sulfonylurea receptor gene in familial persistent hyperinsulinemic hypoglycemia of infancy. Science 268:426–429

Thomas PM, Ye Y, Lightner E (1996) Mutation of the pancreatic islet inward rectifier Kir6.2 also leads to familial persistent hyperinsulinemic hypoglycemia of infancy. Hum Mol Genet 5:1809–1812

Yan F, Lin CW, Weisiger E, Cartier EA, Taschenberger G, Shyng SL (2004) Sulfonylureas correct trafficking defects of ATP-sensitive potassium channels caused by mutations in the sulfonylurea receptor. J Biol Chem 279:11096–11105

Zerangue N, Schwappach B, Jan LY (1999) A new ER trafficking signal regulates the subunit stoichiometry of plasma membrane K_{ATP} channels. Neuron 22:537–548